ADDITIONAL INFORMATION ON METHODS AND RESULTS

$\delta^{18}O$, $\delta^{13}C$, $CaCO_3$ and magnetic susceptibility analyses

The ca. 30 m-thick investigated interval (Fig. DR1) was sampled on the outcropping SUL6 succession with a resolution of ca. 5 cm. Samples were dried in an oven at 60 °C and carbonate content was obtained using gasometry on the bulk samples. A subsample of the dried samples was gently disaggregated and sieved at 100 μm to separate biogenic remains (e.g. ostracods and shells) from the sediments. The fraction below 100 μm was powdered and homogenized. To reduce any additional isotopic effect, no pre-treatment was performed before isotopic analyses following the recommendation of Wierzbowski (2007). Measurements were made using an Analytical Precision AP2003 continuous-flow isotope-ratio mass spectrometer (IRMS) at University of Melbourne, Australia. Samples were digested in 105% phosphoric acid at 70°C. Mass spectrometric measurements were made on the evolved CO_2. Results were normalized to the Vienna Pee Dee Belemnite scale using an internal working standard (NEW1 calibrated against the international standards NBS18 and NBS19). Mean analytical precision on internal standards is ± 0.10 and ± 0.05‰ for the AP2003. Internal reproducibility of the samples is ± 0.15‰.

Low field magnetic susceptibility was measured on whole SUL6 core section (d = 10 cm; Giaccio et al., 2013) every 10 cm with a Bartington MDR2 meter equipped with a MDR2C loop sensor.

$^{40}Ar/^{39}Ar$ dating of tephra layers

Pristine sanidine crystals from SUL2-1, SUL2-7, SUL2-10, SUL2-16 and SUL 2-29 tephra layers from SUL6 unit (Fig. 1) were handpicked under a binocular microscope and then slightly leached for 5 minutes in a 7 % HF acid solution in order to remove groundmass that could be still attached to them. Crystals at both Gif Laboratory and the Berkeley Geochronology Center (BGC) were picked from the same prepared sample for each respective tephra layer. Sample preparation was conducted at Gif laboratory. SUL2-7 was only analyzed at the BGC. SUL2-1, SUL2-16, SUL 2-29 $^{40}Ar/^{39}Ar$ results from Gif Laboratory were already published and discussed in Giaccio et al. (2013) and Sagnotti et al. (2014) and will therefore not be presented in more detail. A summary of both previous and new Gif, BGC, and final combined ages of the dated tephras is provided in Table DR1.

Gif analysis

About 40 crystals were handpicked after leaching and separately loaded in a single well in an aluminum disk and irradiated for 0.5 hours (IRR 50) in the β1 tube of the OSIRIS reactor (CEA Saclay, France). After irradiation, single crystals (300 to 400μm) were individually transferred into a stainless steel sample holder and then loaded into a differential vacuum Cleartran® window. Single crystals were fused at about 15 % of the full laser power using a 25 W CO_2 laser (Synrad®). Ar isotopes were analyzed using a VG5400 mass spectrometer equipped with a single ion counter (Balzers® SEV 217 SEN) following procedures outlined in Nomade et al. (2010). Each Ar isotope measurement consists of 20 cycles of peak switching of the argon isotopes. Neutron fluence (J) was monitored by co-irradiation of 1mm crystals of Alder Creek Sanidine (ACs-2, Nomade et al., 2005) placed in the same pit as the sample. J values were determined from analyses of three ACs-2 single grains for each sample. Procedural blanks were measured every three or four crystals (dataset DR2 in Data Repository). The precision and accuracy of the mass discrimination correction was monitored by daily measurements of air argon at various pressures (see full experimental description in Nomade et al., 2010). Nucleogenic production ratios used to correct for reactor produced Ar isotopes from K and Ca are given in the dataset DR2 and are from Nomade et al., (2014).

BGC analyses

Samples analyzed at the BGC were irradiated for 3 hours (IRR 423 PRA) and 0.5 hours (IRR 412 PRB) in the cadmium-lined CLICIT facility of the TRIGA reactor at Oregon State University. Neutron fluence was monitored by ACs standards bracketing the samples. J-values for each position were determined by the weighted mean of 5-6 analyses each comprising 3-5 grains of ACs. J-values for each of the samples were determined by a planar fit to the standard data.

A MAP 215-50 mass spectrometer with a single analog electron multiplier was used. Data were acquired in 15 cycles of peak-hopping, and relative isotope abundances were determined by regression to an empirically determined equilibration time. Mass discrimination (1.01176 ±0.00106 per dalton) was corrected using the methods described in Renne et al. (2009), based on 37 air pipettes interspersed with the samples and standards. Procedural blanks were measured every 2-3 samples and standards, and their mean and standard deviation were applied for correction. Nucleogenic production ratios used to correct for reactor produced Ar isotopes from K and Ca are given in the dataset DR1.

$^{40}Ar/^{39}Ar$ Results

Detailed information on the $^{40}Ar/^{39}Ar$ dating for individual dated tephra are listed below and shown in Figure DR2 (for the age of the tephras SUL2-15 and SUL2-22 see Table DR1 and related references).

The reported ages are relative to the ACs age of 1.194 Ma (Nomade et al., 2010) and the decay constants of Steiger and Jäger (1977). Combined weighted mean ages and corresponding uncertainties are calculated using IsoPlot 3.0 (Ludwig, 2001) and are given at the 2σ level (analytical uncertainty).

SUL2-1: We combined the previously published results from Gif Sur Yvette Laboratory (Gif) (Giaccio et al., 2013) with the new data from the Berkley Geochronology Center (BCG) acquired in the present study (Table DR1; Fig. DR2). A total of 22 crystals were dated in Gif (Giaccio et al., 2013) and 29 in the BGC for this tephra layer. Ages obtained in the two labs are undistinguishable within uncertainty and were joined to obtain a combined weighted mean age of 724.4 ± 1.6 ka (MSWD = 0.9; P = 0.7) (Fig. DR2).

SUL2-7: A total of 31 crystals were dated at the BGC. Excluding two crystals obviously older, twenty nine crystals are used to calculate a weighted mean age of 749.4 ± 2.6 ka (MSWD = 0.7; P = 0.9) (Fig. DR2).

SUL2-10: 18 and 32 crystals were dated in Gif and the BGC respectively. The results from the two labs are indistinguishable at 95% confidence (Table DR1) and thus they were combined to obtain a weighted mean age of 755.1 ± 1.7 ka (MSWD = 1.2; P = 0.13). Only five older crystals were rejected from the combined weighted mean calculation (Fig. DR2).

SUL2-16: 55 single crystal ages were obtained at the BGC. We combined these results with the data obtained in Gif and already published for the same tephra in Sagnotti et al. (2014) (Table DR1; Fig. DR2). In order to obtain a homogenous population of crystals that is statistically robust, we excluded 29 out of the 55 crystals measured at the BGC. These crystals are clearly statistically older and are the result of xenocrystic contamination. The higher proportion of xenocrysts in the BGC sample probably results from bias in selecting the grains to be analyzed at Gif, as it was the residue of this material that was sent to BGC. A combined weighted mean age based on 52 crystals analyzed in the two laboratories gives 782.2 ± 2.0 ka (MSWD = 0.6; P = 1.0) (Fig. DR2).

SUL2-29: We combined into a single dataset the 39 new $^{40}Ar/^{39}Ar$ single crystal ages obtained at the BGC with the ones already published (Sagnotti et al., 2014; Table DR1) on the same tephra layer. The combined weighted mean age is 807.8 ± 2.3 ka (MSWD = 0.8; P = 0.8) (Fig. DR2; Table DR1).

Table DR1: Gif, BGC and combined $^{40}Ar/^{39}Ar$ ages of the tephras from SUL6 Unit

Tephra	Composite depth (m)	$^{40}Ar/^{39}Ar$ age (ka ± 2σ)		
		Gif	BGC	Combined
SUL 2-1	22.2	724.1 ± 2.0[#]	725.4 ± 3.0*	724.4 ± 1.6
SUL 2-7	26.05		749.4 ± 2.6*	749.4 ± 2.6
SUL 2-10	29.07	754.9 ± 2.6*	760.4 ± 4.1*	755.1 ± 1.7
SUL 2-15	35.35	771.3 ± 2.0[§]	776.8 ± 2.7[§]	773.4 ± 1.6
SUL 2-16	40.8	781.3 ± 2.3[§]	783.0 ± 4.0*	782.2 ± 2.0
SUL 2-22	43.04	792.6 ± 2.5[§]	790.9 ± 2.8[§]	791.9 ± 1.9
SUL 2-29	46.14	810.4 ± 3.1[#, §]	804.0 ± 3.4*	807.8 ± 2.3

* This study; [#] Giaccio et al., 2013; [§] Sagnotti et al., 2014.

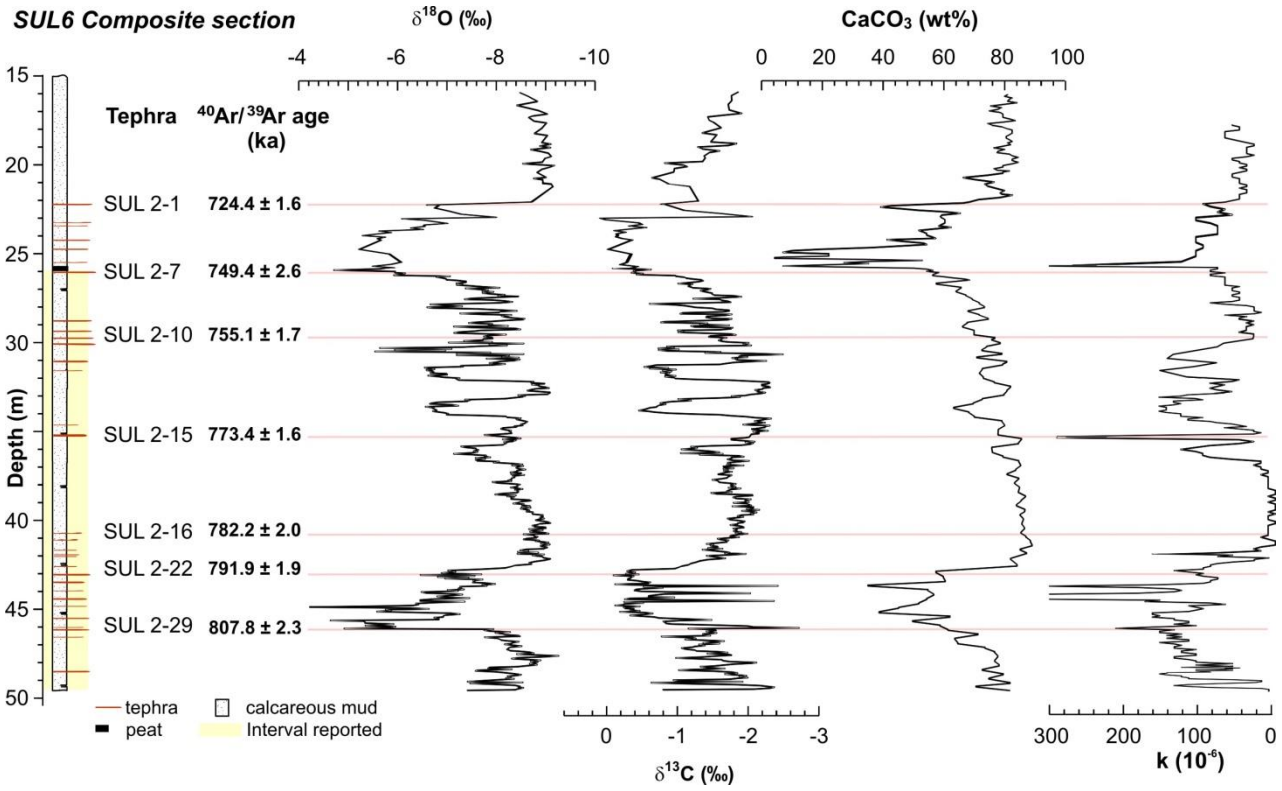

Figure DR1. Depth series ($\delta^{18}O$, $\delta^{13}C$, $CaCO_3$ and magnetic susceptibility [k]) of the investigated Sulmona 6 (SUL6) unit. The yellowish bar, between the depths of ca. 26 m and ca. 49.5 m, represents the stratigraphic interval presented in this study. The position and the ages of the seven $^{40}Ar/^{39}Ar$ dated tephras (pink lines) are also shown.

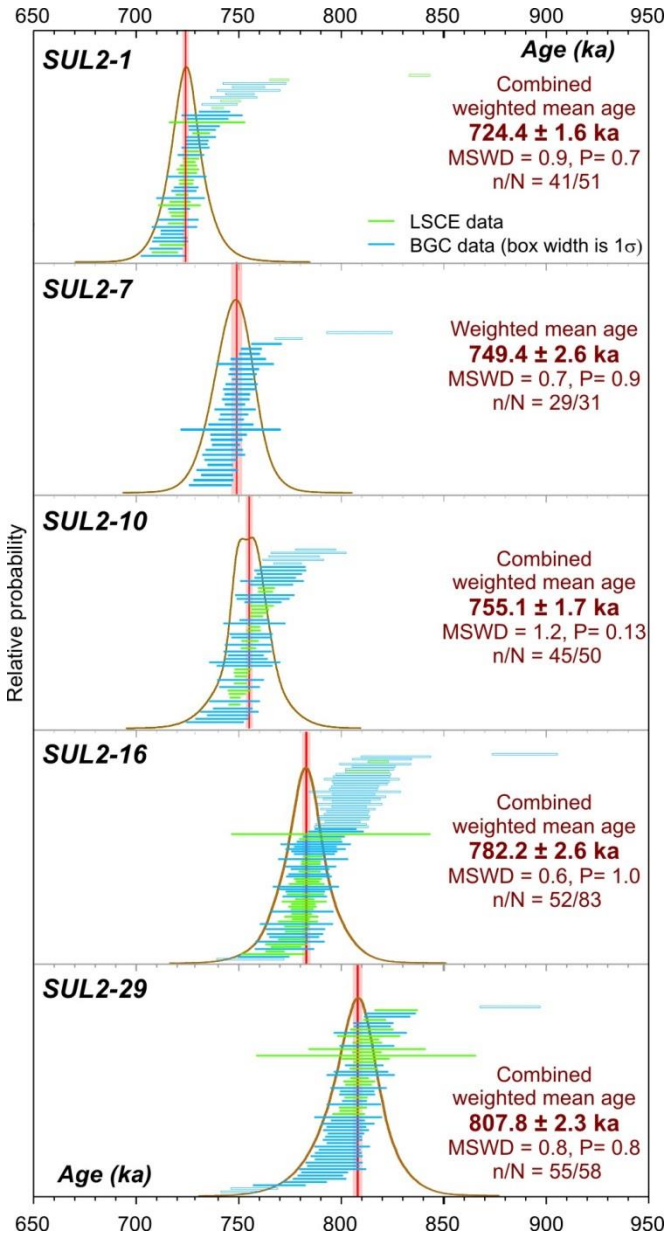

Figure DR2. Age-probability density spectra (2σ analytical uncertainty) and individual crystal age for SUL2-1, SUL2-7, SUL2-10, SUL2-16 and SUL2-29 tephra layers (for the age of the tephras SUL2-15 and SUL2-22 see Table DR1 and related references). Blue and green boxes (1σ) are individual crystals analyzed at the Berkeley Geochronology Center (BGC) and Gif Sur Yvette (LSCE), respectively. Blank boxes are the excluded crystals.

Age Model Parameters

The Bacon age-depth model employed the following parameters: acc.shape = 1.5; acc.mean = 20; mem.strength = 1; mem.mean = 0.1; 121 20cm sections.

REFERENCES CITED

Giaccio, B., Castorina, F., Nomade, S., Scardia, G., Voltaggio, M., and Sagnotti, L., 2013, Revised chronology of the Sulmona lacustrine succession, central Italy; Journal of Quaternary Science, v. 28, p. 545–55.

Ludwig, K.R., 2001. Isoplot 3-A Geochronological Toolkit for Microsoft Excel. Special Publication No 4 Berkeley Geochronology Center (Berkeley), 71 p.

Nomade, S., Gauthier, A., Guillou, H., and Pastre, J.F., 2010, 40Ar/39Ar temporal framework for the Alleret maar lacustrine sequence (French Massif-Central): Volcanological and paleoclimatic implications: Quaternary Geochronology, v. 5, 20–27.

Nomade, S. Pastre, J.F., Guillou H., Faure, M., Guérin, G., Delson, E., Debard, E., Voinchet, P., and Messager. E., 2014, $^{40}Ar/^{39}Ar$ constraints on some French landmark Late Pliocene to Early Pleistocene large mammalian paleofauna: paleoenvironmental and paleoecological implications: Quaternary Geochronology, v. 21, p. 2–15.

Nomade S., Renne, P.R., Vogel, N., Deino A.L., Sharp. W.D., Becker, T.A., Jaouni, A.R., and Mundil, R., 2005, Alder Creek Sanidine (ACs-2): A Quaternary $^{40}Ar/^{39}Ar$ standard: Chemical Geology, v. 218 (3/4), p 319–342.

Renne, P.R., Cassata, W.S., and Morgan, L.E., 2009, The isotopic composition of atmospheric argon and $^{40}Ar/^{39}Ar$ geochronology: time for a change?: Quaternary Geochronology, v. 4, p. 288–298.

Sagnotti, L., Scardia, G., Giaccio, B., Liddicoat, J.C., Nomade, S., Renne, P.R., and Sprain, C.J., 2014, Extremely rapid directional change during Matuyama-Brunhes geomagnetic polarity reversal: Geophysical Journal International, v. 199, p. 1110–1124.

Steiger, R.H., and Jäger, E., 1977, Subcommission on geochronology: convention on the use of decay constants in geo- and cosmochronology: Earth. Planet. Sci. Lett., v. 36, p. 359–362.

Wierzbowski, H., 2007, Effects of pre-treatments and organic matter on oxygen and carbon isotope analyses of skeletal and inorganic calcium carbonate: International Journal of Mass Spectrometry, v. 268, p. 16–29.